Limit cycling in controlled mechanical systems

Limit Cycling in Controlled Mechanical Systems

A Literature Study

Devi Putra

Report No. WFW 2000.038

Professor : Prof.dr. H. Nijmeijer
Coach : Dr.ir. H.A. van Essen

Eindhoven, November 2000

Eindhoven University of Technology
Department of Mechanical Engineering
Section Dynamics and Control

Limit Cycling in Controlled Mechanical Systems
A Literature Study

Devi Putra, M.Sc

November 2000

Contents

Chapter 1

Introduction

In many mechanical systems, limit cycles occur in the form of vibration or oscillation. The term limit cycle refers to an isolated closed orbit in the phase portrait of nonlinear systems. *Limit* indicates the isolated and *cycle* indicates the periodic nature of the motions.

Limit cycling phenomena, which are observed in many mechanical systems, have gained a lot of attention from researchers and engineers for a long time. Recently, as the need of precision positioning systems becomes inevitable, the limit cycle has been the central issue (problem) in precision control designs. A lot of efforts have been done to understand and control the dynamics of the limit cycle. Sophisticated mathematical theories to analyze the dynamics of nonlinear systems, such as topology and bifurcation theory, have been employed to understand more about the limit cycling phenomena.

Radcliffe and Southward investigated the properties of stick-slip friction model that generated limit cycle in [21]. [2] reported that describing function analysis, which is a common approximate technique to analyze limit cycles in nonlinear systems can not describe friction, thus is not a good tool to analyze limit cycle generated by friction. Olsson and Astrom [19] categorized two kinds of friction generated limit cycles, i.e. limit cycle with and without sticking and developed mathematical tools to analyze those limit cycles. Bonsignore et. all. [6] reported pure Coulomb friction plus integral action can produce limit cycles and designed a controller, pole placement technique like. [12] studied bifurcation of friction generated limit cycle under PID controller. Azenha and Machado [3] proposed a first order model variable structure controller (FOM-VSC) that can eliminate friction generated limit cycles with a cost of a small steady-state error. [14] found that fractional derivative (FD) controller outperforms the variable structure controller (VSC).

[3] reported that backlash at the joint of 2R manipulator promotes limit cycles. [7] proposed a delayed feedback controller to eliminate the limit cycle caused by backlash, it successfully used describing function method to analyze the limit cycle and to design the controller. [24] developed a continuous-time adaptive backlash inverse controller that can eliminate limit cycles with a cost of small steady-state error for systems with backlash at their input, and [25] developed an adaptive backlash inverse for systems with backlash at their output. [8] designed a compensation for backlash which is treated as a problem of optimal control. [18] proposed a gear torque compensator and modification of PID controller gains to suppress the backlash generated limit cycle. [15] proposed a hybrid controller to enlarge the basin attraction of the smallest-amplitude limit cycles in the systems with backlash. [1] presented an adaptive backlash inverse controller to suppress the limit cycles caused by backlash and showed that the controller outperforms PD type controllers. [5] proposed a systematic design of a nonlinear controller to decrease the amplitude of limit cycles in the systems with backlash. [22] proposed disturbance observers to suppress limit cycles in a class of nonlinear systems including systems with backlash. [20] analyzed limit cycles and

its bifurcation in a feedback system with dead zone and saturation.

[10] treated friction, backlash, and dead zone as non-smooth nonlinearities, discussed analytical methods for the existence of limit cycles, and proposed a robust tracking controller which is a combination of variable structure controllers and variable structure observers. [23] developed a parameter-space PID controller design method for controlling limit cycles. [4] proposed a feedback control of limit cycle amplitudes in frequency domain. [27] proposed an extremum seeking scheme for limit cycle minimization. [13] discussed how state variables participate in limit cycles behavior. [16] developed a controller for controlling the multiplicity of limit cycles near Hopf bifurcation. [26] discussed harmonic balance analysis of flip bifurcation of limit cycles. And [9] studied codim 1 bifurcation of limit cycles in feedback systems with nonlinearities in the feedback loop and derived simplified conditions for the existence of the bifurcations by using the harmonic balance method.

Chapter 2

Periodic Solutions and Limit Cycles

A solution $x = x(t)$ of continuous-time systems is periodic with least finite period T if $x(t+T) = x(t)$ and $x(t+\tau) \neq x(t)$ for $0 < \tau < T$. For autonomous systems

$$\dot{x} = f(x(t)), \quad x \in R^n \tag{2.1}$$

a periodic solution x of least finite period T corresponds to a closed orbit Γ in R^n and is such that $x(t_0) = x(t_0 + T)$ and $x(t_0 + \tau) \neq x(t_0)$ for $0 < \tau < T$. By specifying the initial time t_0, one specifies a location $x = x_0$ on the orbit. For a periodic solution initiated at $x = x_0$, the positive orbit $\gamma^+(x_0)$ and the negative orbit $\gamma^-(x_0)$ are such that $\gamma^+(x_0) = \gamma^-(x_0) = \Gamma$.

A periodic solution of (2.1) is called a limit cycle if there are no other periodic solutions sufficiently close to it. In other words, a limit cycle is an isolated periodic solution and corresponds to an isolated closed orbit in the phase portrait of the state space. Every trajectory initiated near a limit cycle approaches it either as $t \to \infty$ or as $t \to -\infty$.

Example 1 *Consider the system*

$$\dot{x} = \mu x - \omega y + (\alpha x - \beta y)(x^2 + y^2) \tag{2.2}$$

$$\dot{y} = \omega x + \mu y + (\beta x + \alpha y)(x^2 + y^2) \tag{2.3}$$

where x and y are the states and μ, ω, α, and β are constants.

Under the coordinate transformation

$$x = r\cos\theta \quad \text{and} \quad y = r\sin\theta \tag{2.4}$$

the above system takes the simple form

$$\dot{r} = \mu r + \alpha r^3 \tag{2.5}$$

$$\dot{\theta} = \omega + \beta r^2. \tag{2.6}$$

Multiplying (2.5) with $2r$ yields

$$\frac{d}{dt}(r^2) = 2\mu r^2 + 2\alpha r^4. \tag{2.7}$$

Assuming that $\mu \neq 0$ and using separation of variables, we integrate (2.7) and obtain

$$r = \left[\left(\frac{\alpha}{\mu} + \frac{1}{r_0^2}\right) e^{-2\mu t} - \frac{\alpha}{\mu}\right]^{-1/2} \tag{2.8}$$

where $r_0 \neq 0$ is the value of r at $t = 0$. Letting $\theta = \omega t + \phi$ in (2.6) gives

$$\dot{\phi} = \beta r^2. \tag{2.9}$$

Then, it follows from (2.7) and (2.9) that

$$\frac{d\phi}{dr^2} = \frac{\beta}{2\mu + 2\alpha r^2} \tag{2.10}$$

when $r^2 \neq -\mu/\alpha$. Hence, for $\alpha \neq 0$,

$$\phi = \frac{\beta}{2\alpha} \ln(2\mu + 2\alpha r^2) + c \tag{2.11}$$

where c is a constant. Substituting for r and θ in (2.4), we obtain a closed-form solution of (2.2) and (2.3).

When $\mu > 0$ and $\alpha < 0$, it follows from (2.8) that

$$\lim_{t\to\infty} r = (-\mu/\alpha)^{1/2}$$

irrespective of the value r_0 as long as it is different from zero. Consequently, it follows from (2.6) that

$$\lim_{t\to\infty} \dot{\theta} = \omega - \beta\mu/\alpha. \tag{2.12}$$

Therefore, we have

$$\lim_{t\to\infty} x = (-\frac{\mu}{\alpha})^{1/2} \cos[(\omega - \frac{\beta\mu}{\alpha})t + \theta_0] \tag{2.13}$$

$$\lim_{t\to\infty} y = (-\frac{\mu}{\alpha})^{1/2} \sin[(\omega - \frac{\beta\mu}{\alpha})t + \theta_0] \tag{2.14}$$

where θ_0 is the initial value of θ. Equations (2.13) and (2.14) represent a closed orbit in the $x - y$ plane. This orbit is a circle whose center is at origin and radius is $\sqrt{-\mu/\alpha}$; that is,

$$x^2 + y^2 = -\mu/\alpha. \tag{2.15}$$

The closed orbit in Figure 2.1a corresponds to the periodic solution of (2.2) and (2.3) when $\mu > 0$ and $\alpha < 0$. The figure also displays four positive orbits with the arrow on each of the orbit indicating the direction of evolution. Since there are no other closed orbit sufficiently near this periodic solution (in fact, there is no other closed orbit in the entire planar space), the closed orbit of Figure 2.1a is a limit cycle. It is also an invariant set because an orbit initiated from any point on the closed trajectory remains on this orbit for all times. Furthermore, we observe that positive orbits initiated from different points in the state space $x - y$, other than origin are attracted to the limit cycle. Hence, it is a stable limit cycle or a periodic attractor. Its basin of attraction is the entire $x - y$ space excluding the origin, which is an unstable fixed point of (2.2) and (2.3).

When $\mu < 0$ and $\alpha > 0$, we infer from (2.8) that

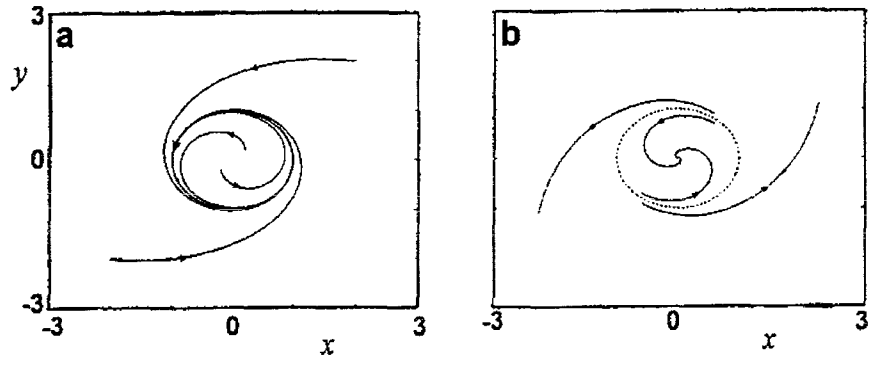

Figure 2.1: Periodic solutions of (2.2) and (2.3)

$$\lim_{t\to-\infty} r = (-\mu/\alpha)^{1/2}.$$

Then, (2.15) still describes the corresponding closed orbit in the $x-y$ plane. In Figure 2.1b, we show some orbits of (2.2) and (2.3) when $\mu < 0$ and $\alpha > 0$. Here, the closed orbit is depicted by broken lines. Again, because there are no other closed trajectories sufficiently near this periodic solution, it is a limit cycle. Further, it is also an invariant set. Moreover, this limit cycle is said to be unstable because all positive orbits initiated from nearby points spiral away from it as $t \to \infty$ while all negative orbits initiated from nearby points spiral toward it as $t \to -\infty$. In Figure 2.1b, the origin is a point attractor of (2.2) and (2.3), and its basin of attraction is bound by the closed orbit.

Example 2 *We consider the system*

$$\ddot{x} + x + 2x^3 = 0. \tag{2.16}$$

Multiplying (2.16) with $2\dot{x}$ and integrating , we obtain

$$\dot{x}^2 + x^2 + x^4 = H = \dot{x}_0^2 + x_0^2 + x_0^4. \tag{2.17}$$

where H is a constant that represents the total energy of the system and $x_0 = x(0)$, and $\dot{x}_0 = \dot{x}(0)$. Thus, for any initial condition $(x_0, \dot{x}_0)$, (2.17) represents a closed trajectory in the $\dot{x} - x$ plane and, hence, a periodic solution. In Figure 2.2, we show four closed orbits of (2.16) obtained by choosing four different initial conditions. It is noticed that periodic solutions in Figure 2.2 are not isolated but form a continuum. Because there exist an infinite number of closed trajectories in the vicinity of any closed trajectory, a periodic solution of (2.16) is not a limit cycle.

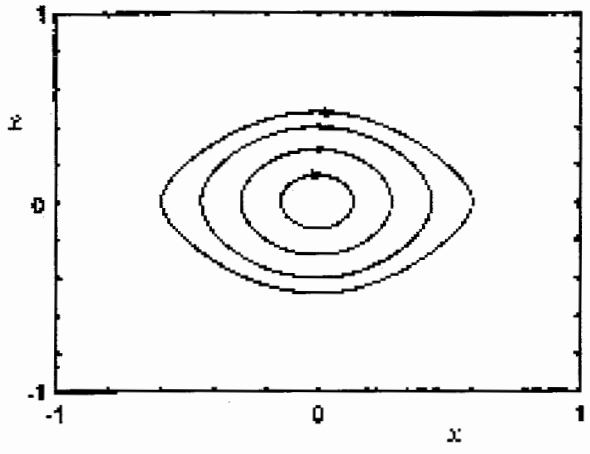

Figure 2.2: Periodic solutions of (2.16)

Chapter 3

Mechanical Systems that Exhibit Limit Cycles

3.1 Mechanical Systems with Friction

Radcliffe and Southward [21] investigated the properties of stick-slip friction model that generated limit cycle. They investigated the controlled stick-slip mass as shown in Figure 3.1. Some friction models, which are shown in Figure 3.2, were used. It is shown that limit cycles only occur for the friction models whose damping function drops (dis)continuously for non-zero velocity from the static force level (i.e. the Stiction plus Viscous Model and Exponential plus Viscous Model in Figure 3.2, and the controller must have an integral action.

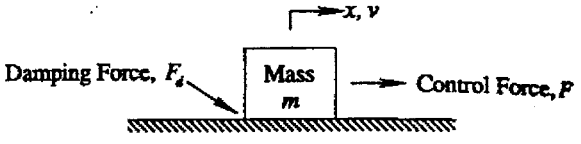

The 1-DOF conceptual stick-slip mass system used to investigate models of stick-slip friction force.

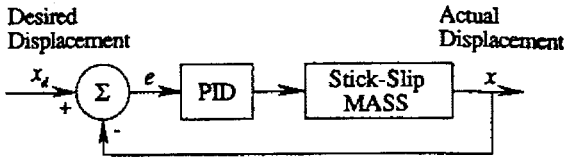

Block Diagram of PID control system incorporating stick-slip mass system.

Figure 3.1: Controlled stick-slip mass system

Bonsignore et. all. [6] reported pure Coulomb friction plus integral action can also produce limit cycles. The the stick-slip models induce limit cycle with sticking, where the velocity at the friction interface is zero during a time interval. While the pure Coulomb friction model induces limit cycle without sticking, the velocity is zero only at isolated time instants. The last type of limit cycle can be explained in the terms of relay oscillations. It

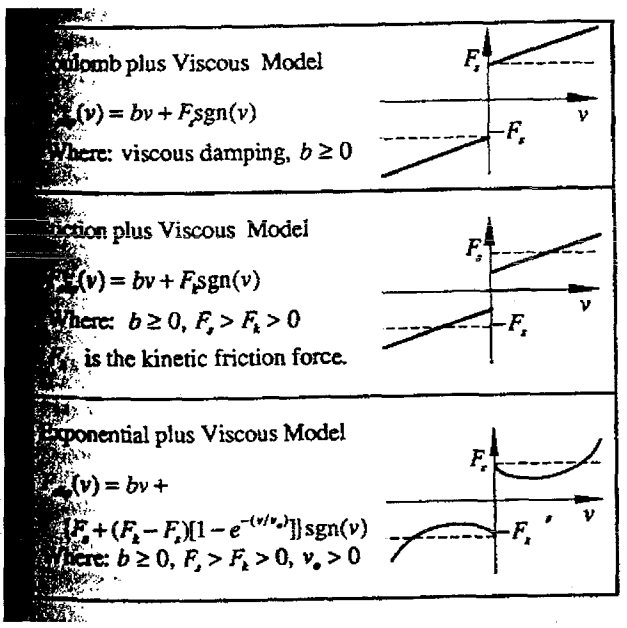

Figure 3.2: Three friction models

is shown in [2] that the describing function method, which is explained in section 4.1, is not a good method to analyze friction induced limit cycles because the friction induced limit cycle often can not be approximated by a nonbiased sinusoidal function.

3.2 Mechanical Systems with Backlash

Backlash occurs in mechanical systems driven via two mating masses (gears) as depicted in Figure 3.3b. In Figure 3.3b the movement of the driving gear is denoted by $v(t)$, and the position of the driven gear is denoted by $u(t)$, while the slope m depends on the ratio of the mass of the two gears.

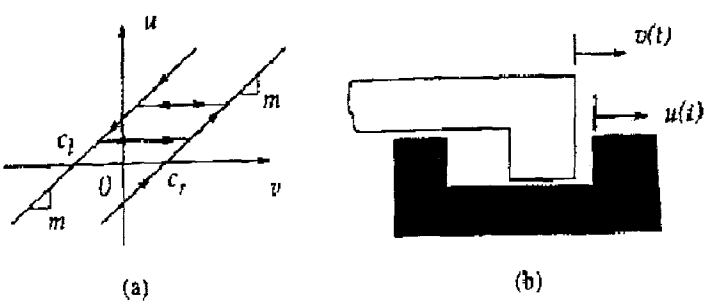

Figure 3.3: Backlash model

The mathematical model of the backlash is given by

$$u = \begin{array}{ll} m(v - c_r) & if \;\; \dot{v}(t) > 0 \; and \; u(t) = m(v(t) - c_r) \\ m(v + c_l) & if \;\; \dot{v}(t) < 0 \; and \; u(t) = m(v(t) + c_l) \\ u & otherwise \end{array} . \tag{3.1}$$

Another way to model backlash is using the principle of conservation of momentum after collision, yields a dynamic model of backlash. Let the two mating gears have masses M_1 and M_2 respectively, x_1 and x_2 are their position respectively, and the clearence between the two gears is h_1. A collision between the masses M_1 and M_2 occurs when $x_1 = x_2$ or $x_2 = x_1 + h_1$. In this case, we can compute the velocities of masses M_1 and M_2 after the impact ($\dot{x}_1'$ and $\dot{x}_2'$, respectively) by applying the Newton's law

$$\dot{x}_{12}' = -\varepsilon \dot{x}_{12}, \;\; 0 \leq \varepsilon \leq 1 \tag{3.2}$$

where $x_{12} = x_1 - x_2$, and ε is the restitution coefficient. On the other hand, by the principle of conservation of momentum it comes

$$M_1 \dot{x}_1' + M_2 \dot{x}_2' = M_1 \dot{x}_1 + M_2 \dot{x}_2. \tag{3.3}$$

From equations (3.2) and (3.3), we obtain

$$\dot{x}_1' = \frac{\dot{x}_1(M_1 - \varepsilon M_2) + \dot{x}_2(1 + \varepsilon)M_2}{M_1 + M_2} \tag{3.4}$$

$$\dot{x}_2' = \frac{\dot{x}_1(1 + \varepsilon)M_1 + \dot{x}_2(M_2 - \varepsilon M_1)}{M_1 + M_2}. \tag{3.5}$$

It is reported in [3] that backlash at the joint of a 2R manipulator promotes limit cycles. [3] also showed that the describing function method can predict the limit cycles with a very good accuracy in terms of frequency of the oscillation.

3.3 Servo Systems with Dead Zone and Saturation

Ortega et. all. [20] reported that a dc servomechanism with proportional gain controller exhibits limit cycle due to the deadzone and saturation in the characteristic map of the input voltage to the output velocity of the dc motor. The block diagram of the system and the nonlinear input-output relation can be seen in Figure 3.4 and Figure 3.5, respectively.

The deadzone in Figure 3.4 due to static friction between rotor and stattor of the dc motor, while the saturation is caused by the magnetic field saturation. In Figure 3.5, $G(s)$ is the linear transfer function of the dc motor and K_c is the proportional gain.

It is noted that in such a system the high frequency dynamic of the linear part of the model of the system, $G(s)$, plays an important role to explain the occurence of the limit cycles. The high-frequency pole of $G(s)$ is usually not identified via indentification using temporal response to a step input. [20] shows that the limit cycle of this type of system can be predicted and analyzed by using the describing function method, see section 4.1. The limit cycle occurs at a certain value of controller gain, $K_c = K_c^{\min}$. For $K_c < K_c^{\min}$ there is no limit cycle occured, instead the system has a band of stable fixed (equilibrium) points including origin. But for $K_c > K_c^{\min}$ the system has two limit cycles and the band of stable fixed points. The limit cycle with bigger amplitude is stable, while the smaller one is unstable. This lead to the fold bifurcation of limit cycles with the controller gain K_c is the bifurcation parameter. The bifurcation of limit cycles is explained in Chapter 6.

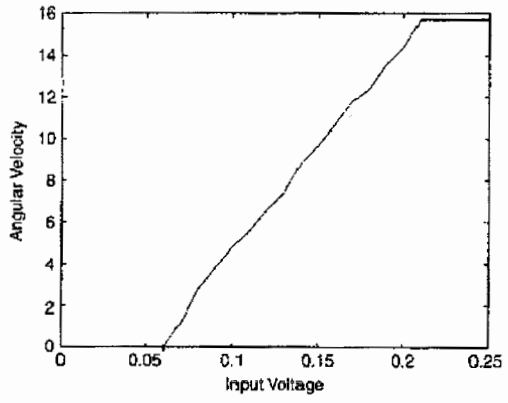

Figure 3.4: Static characteristic of the servomechanism for positive values input

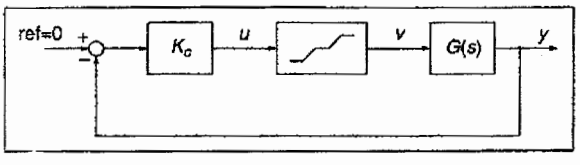

Figure 3.5: The closed loop system with proportional gain

Chapter 4

Tools for Predicting Limit Cycles

4.1 Analytical Tools

4.1.1 Describing Functions

The describing function technique is a frequency response method. This method is applied for nonlinear systems that can decomposed into linear subsystems and a nonlinear subsystem, which can be depicted by Figure 4.1. In the figure 4.1 G_1 and G_2 represent linear parts of the system and N is a nonlinear element.

In the describing function analysis, it is assumed that the input x to the nonlinearity is sinusoidal

$$x = A \sin \omega t \tag{4.1}$$

and the linear subsystems have a low pass filter characteristic. This method works as follows. Let the nonlinear element be an ideal relay. As shown in Figure 4.2, the square wave is the output of an ideal relay for a sinusoidal input. The square wave can be represented by a Fourier series of the general form

$$y(t) = b_0 + \sum_{n=1}^{\infty} (a_n \sin n\omega t + b_n \cos n\omega t). \tag{4.2}$$

Since G_2 is assumed to be a low pass filter then the harmonic terms ($n > 1$) can be

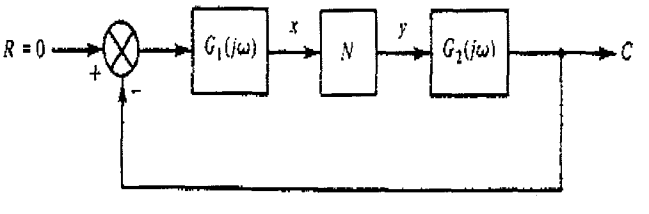

Figure 4.1: System configuration for Describing Function analysis

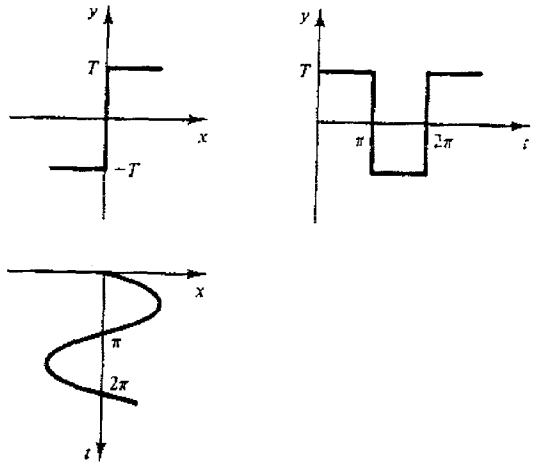

Figure 4.2: Square-wave output of ideal delay element given sinusoinal input

neglected. Thus, the output y is approximated by the fundamental Fourier component

$$y_f = a_1 \sin \omega t + b_1 \cos \omega t. \tag{4.3}$$

Hence, the nonlinear element can be modelled as a function

$$N = \frac{y_f}{x} \tag{4.4}$$

which is called describing function. Since N is modelled as an equivalent linear gain, in Figure 4.1 , for $R = 0$ (because limit cycle is a self-sustained oscillation), we have

$$C(GN + 1) = 0 \tag{4.5}$$

where $G = G_1 G_2$ is the product of linear elements in the loop. From (4.5), the condition for existence of a nonzero solution (limit cycle) for the output C is

$$GN + 1 = 0 \text{ or } G = -1/N. \tag{4.6}$$

This has a graphical interpretation that a limit cycle is identified by the intersection of the polar plot of $G(j\omega)$ and a plot of $-1/N$. Furthermore, the predicted limit cycle has amplitude A and angular frequency ω.

4.1.2 Harmonic Balance

Harmonic balance method basically is the same as the describing function. In this method the periodic output y is approximated not only by the fundamental Fourier component but with some harmonic terms in addition to the fundamental Fourier component.

4.2 Numerical Computation

4.2.1 Shooting Method

The periodic solution of the nonlinear systems $\dot{x} = f(x)$ is found by solving 2-points boundary value problem, in which the solutions are sought of

$$H(x,T) \equiv \phi_T(x) - x = 0, \tag{4.7}$$

where T is the period of the periodic solution. Since (4.7) is a system of n equations with $n+1$ unknowns (the n components of x and period T) can not be solved directly. Instead, $y \equiv H(x,T)$ is linearized, to obtain

$$\Delta y \approx \frac{\partial H}{\partial x}\Delta x + \frac{\partial H}{\partial T}\Delta T = (\Phi_T(x) - I)\Delta x + f(\phi_T(x))\Delta T \tag{4.8}$$

where $\Phi_T(x)$ is the solution of the variational equation. To achieve $H \approx 0$, Δx and ΔT are chosen such that $\Delta y = -H$. This value of Δy is substituted to (4.8), yields

$$-H = (\Phi_T(x) - I)\Delta x + f(\phi_T(x))\Delta T. \tag{4.9}$$

In order to make this system solvable, a constraint is added, which restrict the state correction term Δx to be orthogonal to $f(x)$, given by

$$f(x)^T \Delta x = 0. \tag{4.10}$$

From (4.9) and (4.10), the following iterative scheme is assembled, with which zeros of H can be found, using initial guesses $x^{(0)}$ and $T^{(0)}$.

$$\begin{bmatrix} \Phi_{T^{(i)}}(x^{(i)}) - I & f(\phi_{T^{(i)}}(x^{(i)})) \\ f(x^{(i)})^T & 0 \end{bmatrix} \begin{bmatrix} \Delta x^{(i)} \\ \Delta T^{(i)} \end{bmatrix} = \begin{bmatrix} x^{(i)} - \phi_{T^{(i)}}(x^{(i)}) \\ 0 \end{bmatrix} \tag{4.11}$$

$$\begin{bmatrix} x^{(i+1)} \\ T^{(i+1)} \end{bmatrix} = \begin{bmatrix} x^{(i)} \\ T^{(i)} \end{bmatrix} + \begin{bmatrix} \Delta x^{(i)} \\ \Delta T^{(i)} \end{bmatrix} \tag{4.12}$$

where the superscript indicates the iteration count. This scheme is reiterated until some convergence criteria is met. The algorithm is similar to the Newton-Raphson algorithm, and thus the same convergence property is applied. When the shooting method returns values $\hat{x}$ and $\hat{T}$, it should be tested whether $\hat{T}$ is the minimum period of the solution, since it could be a multiple of the actual period.

Chapter 5

Available Control Schemes

This chapter presents some available control schemes for eliminating, reducing amplitude, and controlling the amplitude and frequency of limit cycles. Most of the control schemes are designed for controlling limit cycles induced by a certain type of nonliniearity.

5.1 Compensation Techniques

In this section, we present some methods to eliminate or reduce the size of limit cycles by designing a compensator to eliminate the nonlinear element that induces the limit cycles.

5.1.1 Compensation for Backlash

Tao and Kokotovic [24] developed an adaptive backlash scheme and applied it to feedback control of a known linear plant and unknown backlash at its input. In this case, backlash as depicted in Figure 3.3 is modelled as

$$\dot{u}(t) = \begin{cases} m\dot{v}(t) & if \ \dot{v}(t) > 0 \ and \ u(t) = m(v(t) - c_r) \\ & or \ \dot{v}(t) < 0 \ and \ u(t) = m(v(t) + c_l) \\ 0 & otherwise \end{cases}, \tag{5.1}$$

which is a time derivative of backlash model (3.1) in section 3.2.

The desired function of a backlash inverse is to cancel the damaging effects of backlash on system performance: the delay corresponding to time needed to traverse an inner segment of $B(\cdot)$ and the information loss occuring on an inner segment when the output $u(t)$ remains constant while the input $v(t)$ continues to change. That is, given a desired signal $u_d(t)$ for $u(t)$, a backlash inverse $BI(\cdot)$ is such that $u_d(t) = B(BI(u_d(t)))$, see Figure 5.1.

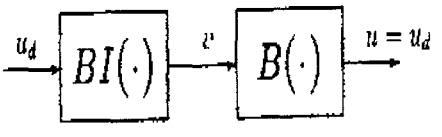

Figure 5.1: Backlash inverse for compensation

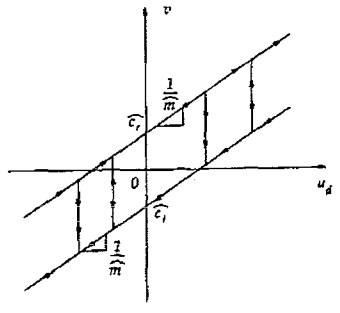

Figure 5.2: Adaptive inverse backlash

The following mapping $BI(\cdot) = BI(m, c_r, c_l; \cdot)$ from $u_d(t)$ to $v(t)$ defines such a backlash inverse:

$$\dot{v}(t) = \begin{cases} \frac{1}{m}\dot{u}_d(t) & if\ \dot{u}_d(t) > 0\ and\ v(t) = \frac{u_d(t)}{m} + c_r \\ & or\ \dot{u}_d(t) < 0\ and\ v(t) = \frac{u_d(t)}{m} + c_l \\ 0 & if\ \dot{u}_d(t) = 0 \\ g(t,t) & if\ \dot{u}_d(t) > 0\ and\ v(t) = \frac{u_d(t)}{m} + c_l \\ -g(t,t) & if\ \dot{u}_d(t) < 0\ and\ v(t) = \frac{u_d(t)}{m} + c_r \end{cases} \tag{5.2}$$

where $g(\tau, t) = \delta(\tau - t)(c_r - c_l)$ with $\delta(t)$ being the Dirac δ-function. In this definition the inverse of a horizontal segment of the backlash characteristic is a vertical jump of a distance $c_r - c_l$.

When the exact backlash parameters are unknown, we use their estimates $\hat{m}(t)$, $\hat{c}_r(t)$, $\hat{c}_l(t)$ to design an adaptive backlash inverse $\hat{BI}(\cdot) \triangleq \hat{BI}(\hat{m}, \hat{c}_r, \hat{c}_l; \cdot)$, which is graphically depicted in Figure 5.2 by two parallel straight lines and instantaneous vertical transitions between this two lines. The instantaneous vertical transitions take place whenever $\dot{u}_d(t)$ changes its sign.

5.1.2 Disturbance Observer

Shahruz and Rajarama [22] designed disturbance observers to suppress limit cycles in a class of nonlinear feedback systems. The class of nonlinear feedback systems are those that can be decomposed into a linear plant, P, and a nonlinearity, N, which are shown in Figure 5.3.

The nonlinear systems in Figure 5.3 is called $S(N, P)$ systems, which consist of the plant P represents a (possibly unstable) SISO linear time-invariant system, the nonlinearity N represents a SISO nonlinear time-varying system that can be decomposed as

$$N = H + \Phi \tag{5.3}$$

where H is a stable SISO linear time-invariant system, and Φ is a SISO time-varying nonlinearity, whose output is given by

$$d(t) := (\Phi u)(t) = \phi(u(t), t). \tag{5.4}$$

It is assumed that d is bounded for any bounded input u. The C in Figure 5.3 is a SISO linear or nonlinear controller that at least achieves the BIBO stability of the system $S(N, P)$.

By equations (5.3) and (5.4), the output of the nonlinearity N is the summation of the output of a stable linear time-invariant system and a bounded function of time, i.e:

$$\eta(t) = (Nu)(t) = (Hu)(t) + d(t). \tag{5.5}$$

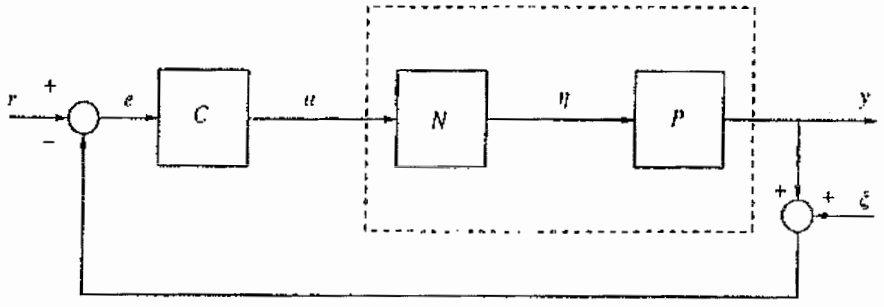

Figure 5.3: Nonlinear feedback system $S(N, P)$

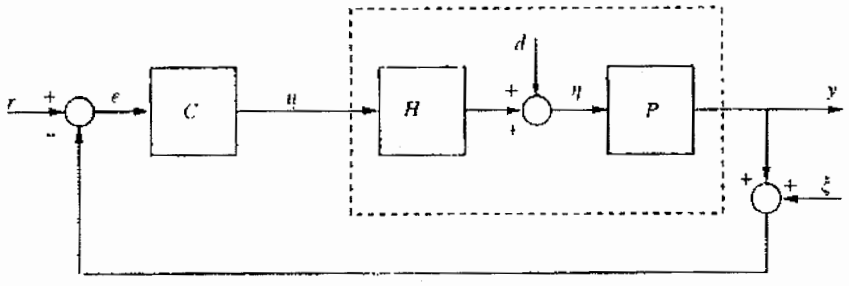

Figure 5.4: The equivalent feedback system $S(H, P)$

Under the above decomposition the $S(N, P)$ system can be transformed into $S(H, P)$ system, which is an equivalent from the input-output point of view. The controlled $S(H, P)$ system is depicted in Figure 5.4.

The disturbance observer is designed to suppress the effect of the bounded disturbance d in the $S(H, P)$ system, which is depicted in Figure 5.5.

In Figure 5.5, $H_n(s)$ and $P_n(s)$ represent the nominal transfer function of $H(s)$ and $P(s)$ respectively, and $Q(s)$ is a low-pass filter with the unity DC-gain. A typical form of $Q(s)$ is

$$Q(s) = \frac{\sum_{k=1}^{m-\rho} a_k(\tau s)^k + 1}{\sum_{k=1}^{m} a_k(\tau s)^k + 1}, \tag{5.6}$$

where ρ is at least equal to the summation of the relative degrees of $H_n(s)$ and $P_n(s)$, and a_k and τ are positive real numbers. A realizable implementation of the disturbance observer for the system $S(N, P)$ (equivalently $S(H, P)$) is shown in Figure 5.5. [22] showed that the disturbance observer successfully eliminates the backlash induced limit cycles.

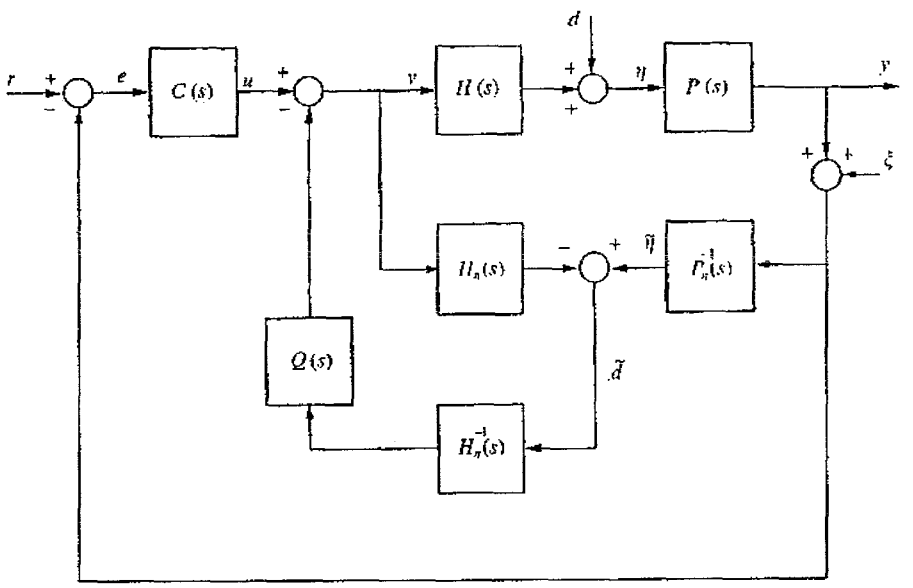

Figure 5.5: The $S(H,P)$ system with disturbance observer

5.2 Variable Structure Controller (VSC)

[3] applied the VSC, expressed by the following equation, to a 2R manipulator.

$$\tau = \begin{array}{ccc} \tau_{\max} & \text{if} & \sigma \geq \tau_{\max}/K \\ K\sigma & \text{if} & |\sigma| < \tau_{\max}/K \\ -\tau_{\max} & \text{if} & \sigma \geq \tau_{\max}/K \end{array} \tag{5.7}$$

The VSC becomes of first order, First Order Model (FOM) VSC, if the sliding surface σ obeys the expression:

$$\sigma = \dot{q}_e + cq_e \tag{5.8}$$

where the parameter c is the corresponding eigenvalue, q_e is the input to the VSC and τ is the respective output. For a second order model (SOM) VSC, the sliding surface σ is given by

$$\sigma = \ddot{q}_e + 2\zeta\omega_n\dot{q}_e + \omega_n^2 q_e \tag{5.9}$$

where ζ is the damping ratio. The block diagram of the VSC is shown in Figure 5.6.

[3] showed that the VSC can eliminate the friction induced limit cycle with the cost of a small steady-state error but does not succeed to eliminate backlash induced limit cycle.

5.3 Fractional Derivative (FD) controller

FD controller is a proportional derivative (PD) controller like where the term derivative, $\frac{d}{dt}$, is replaced by fractional derivative which is defined as follows. The fractional derivative of order α, D^α :

$$D^\alpha\, x(t) = \lim_{h\to 0}\left[\frac{1}{h^\alpha}\sum_{k=0}^{\infty}(-1)^k \frac{\Gamma(\alpha+1)}{\Gamma(k+1)\Gamma(\alpha-k+1)} x(t-kh)\right] \tag{5.10}$$

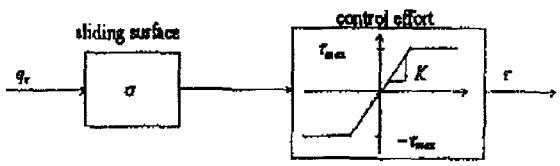

Figure 5.6: Block diagram of the VSC

where Γ is the gamma function and h is the time increment. Therefore, for a discrete-time control algorithm, with sampling period T, this formula can be approximated through a r-th order truncated series, resulting the following equation in z-domain:

$$Z\{D^{\alpha}\, x(t)\} \approx \left\{ \frac{1}{T^{\alpha}} \sum_{k=0}^{r} (-1)^{k} \frac{\Gamma(\alpha+1) z^{-k}}{k!\Gamma(\alpha-k+1)} \right\} X(z). \tag{5.11}$$

In order to have a good approximations, we must have a large number of terms and a small sampling period.

[14] compared the performance of the FD controller and the VSC controller in stabilizing a 2R manipulator having backlash, friction, and flexibility in the joints, which can exhibits limit cycling. It turns out that the FD controller outperforms the VSC controller in suppressing limit cycles.

Chapter 6

Bifurcation of Limit Cycles

Bifurcation theory is concerned with the qualitative changes in the phase portrait of a system as a result of the birth or the disappearance of limit sets and their corresponding basins. Since limit cycle is one of these limit sets, the birth, and the disappearance of the limit cycles causes bifurcations in the dynamics of a system. Bifurcations of limit cycles refer to any qualitative changes with respect to limit cycles, i.e. the birth, the disappearance, the multiplicity, and the change of stability of the limit cycles.

There are four kinds of bifurcations of limit cycles, which will be presented in the following sections.

6.1 Hopf Bifurcation

In the Hopf bifurcation of limit cycles is born from equilibrium (stationary solutions) at the bifurcation point (Hopf point) because the equilibrium after the bifurcation point becomes unstable. The scenarios of this type of bifurcation can be seen in Figure 6.1.

In Figure 6.1a, the branch of stationary solutions extends beyond λ_0, but it is unstable for $\lambda > \lambda_0$. The Jacobian at a Hopf bifurcation has a pair of purely imaginary eigenvalues $\pm i\beta$. Here a branch of periodic orbits is born. It is also noticed in the Figure 6.1a, that for $\lambda > \lambda_0$, $\lambda \to \lambda_0$ the periodic solutions merge into the stationary branch, the amplitude vanishes. The bifurcation is vertical and the amplitude locally behaves like $\sqrt{|\lambda > \lambda_0|}$.

The situation in of Figure 6.1a and Figure 6.1b depicts a transition without jump: passing λ_0 when increasing λ one experience *a soft loss* of stability of the stationary state; the bifurcation is *supercritical.* Figure 6.1c illustrates a *subcritical* situation where locally no stable exists for $\lambda > \lambda_0$. Globally, this local scenario often extends to a different situations, see Figure 6.1d.

In Figure 6.1d the branch of unstable periodic orbits bends back, gaining stability at a turning-point-like situation. Consequently, when we increase λ beyond the critical Hopf parameter value λ_0 a jump occurs. For $\lambda > \lambda_0$, there are no neighboring small-amplitude periodic solutions, and the dynamics is immediately attracted by a large-amplitude limit cycles. This large jump is the *hard loss* of stability.

6.2 Fold Bifurcation

Fold bifurcation occurs if a branch of stable limit cycles and a branch of unstable limit cycles collide and disappear at the bifurcation point. Figure 6.2 shows that for bifurcation parameter $\alpha < 0$ the system has two limit cycles; a stable limit cycle L_1 and an unstable limit cycle L_2. As the bifurcation parameter α increases, at the bifurcation point $\alpha = 0$ the

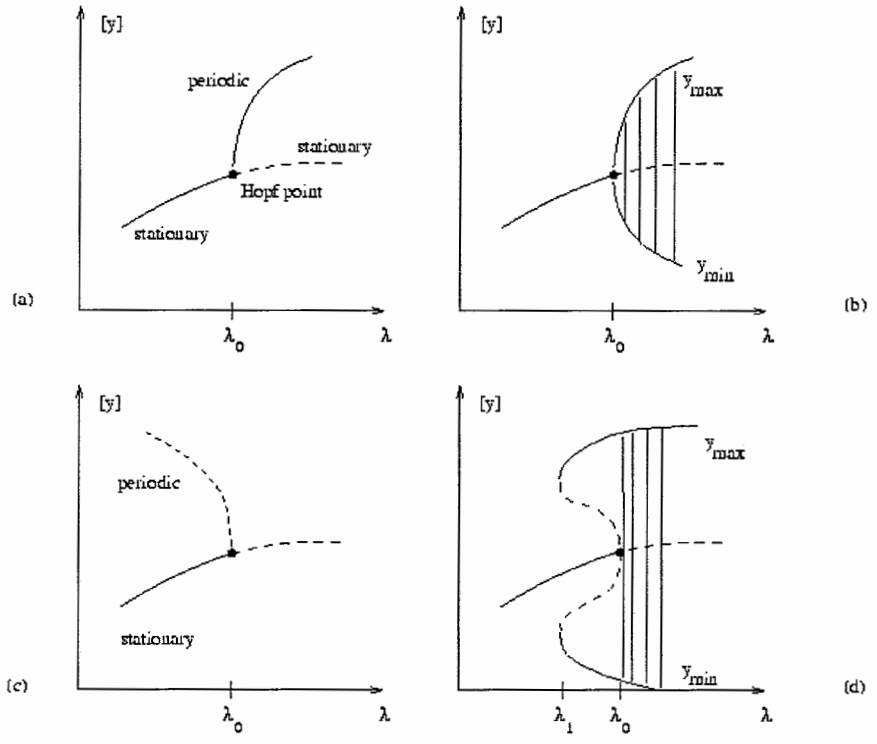

Figure 6.1: Scenario of Hopf bifurcation of lmit cycle

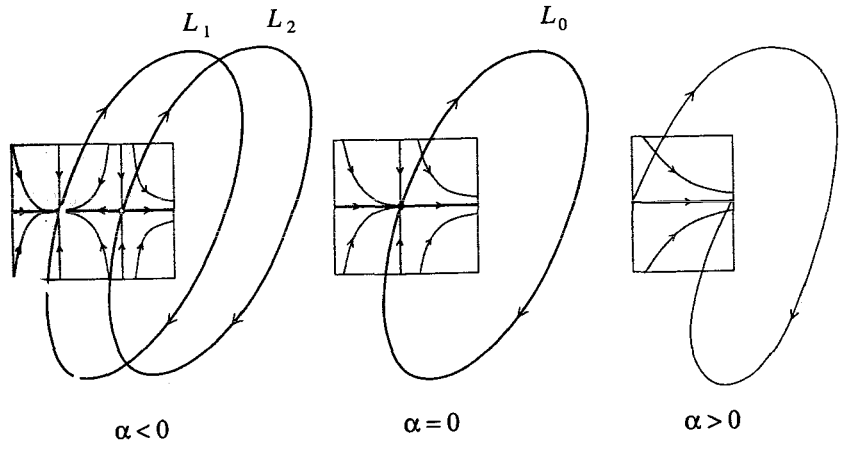

Figure 6.2: Fold bifurcation of limit cycles

two limit cycles merge and form a semi-stable limit cycle L_0. For $\alpha > 0$, the limit cycle L_0 disappears, thus the system has stationary solutions.

6.3 Flip Bifurcation

In a flip bifurcation (also called period doubling), a cycle of period two (a stable limit cycle) appears and the current branch of limit cycle loses stability. This situation can be seen in Figure 6.3.

Dynamically, the flip bifurcation is the following scenario (see Figure 6.4): Assume a branch of periodic solutions (limit cycles) parameterized by λ with stable orbits on one side of (say, $\lambda < \lambda_0$) and a multiplier crossing the unit circle with $\mu(\lambda_0) = -1$. Then, locally, there are periodic orbits with the double period near λ_0. These double-periodic orbits form a new branch that emerges at λ_0. Note that the periods vary with λ, and the factor 2 of period doubling holds only asymptotically for $\lambda \to \lambda_0$. The situation typically is as in the left part of Figure 6.4, for $\lambda_0 = \lambda_{01}$. The *new* branch of the *double* period can experience a period doubling too, and forms a cascade of period doubling as shown in Figure 6.4. In the supercritical case, the stability is exchanged to the branches of the double period. After some period doublings the period has become so large that the orbit looks irregular. It has been shown that the bifurcation values satisfy a universal scaling law,

$$\lim_{v\to\infty} \frac{\lambda_{v+1} - \lambda_v}{\lambda_v - \lambda_{v-1}} = 0.214169... \tag{6.1}$$

This scaling law, named after Feigenbaum, has a remarkable consequence: There is an accumulation point λ_∞ of the sequence of period doubling bifurcations. Passing λ_∞ means that the "period" has reached infinity. The resulting solution is fully aperiodic, and is chaotic. It is well known that a cascade of period doubling is one of the important routes to chaos.

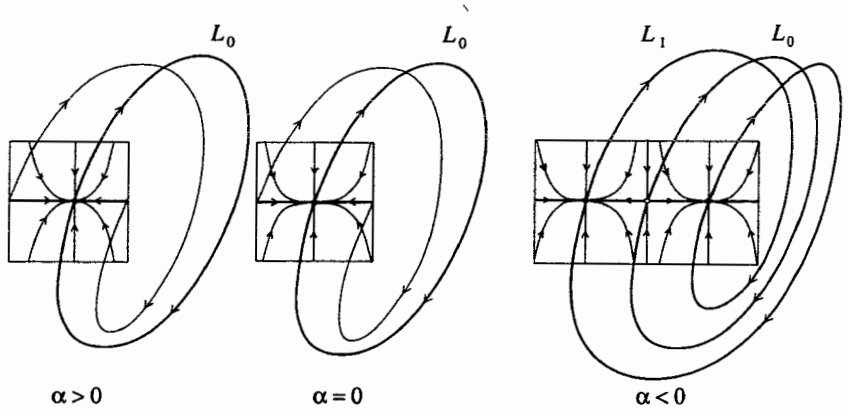

Figure 6.3: Flip bifurcation of limit cycles

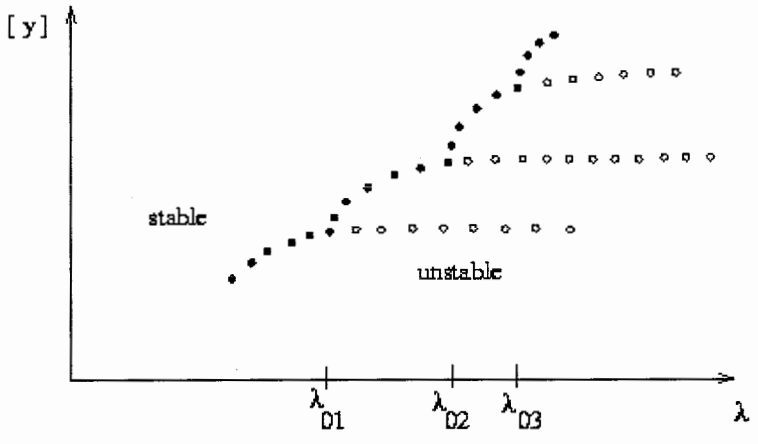

Figure 6.4: Cascade of period doubling bifurcation

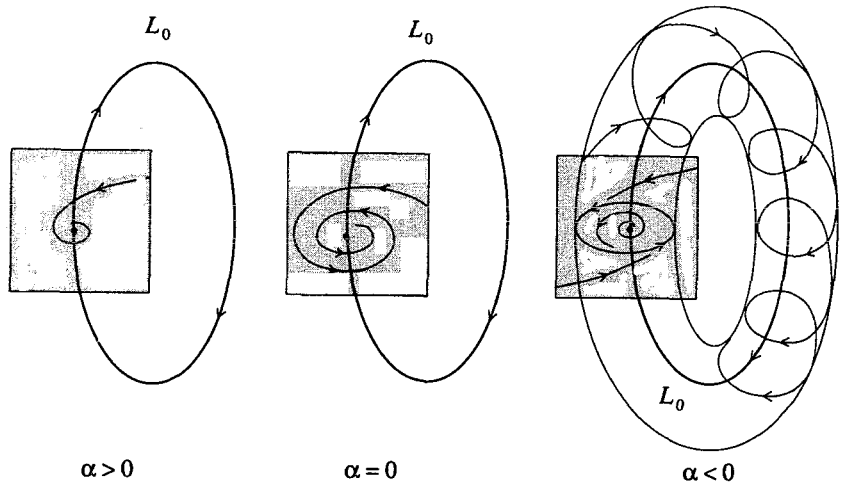

Figure 6.5: Neimark-Sacker bifurcation of limit cycles

6.4 Neimark-Sacker Bifurcation

In Neimark-Sacker bifurcation some long-period cycles of difference stability appear on a two-dimensional invariance torus, as depicted in Figure 6.5. Its scenario is as follows. For the bifurcation parameter $\alpha > 0$, the system has a stable limit cycle L_0. As α decreases until it reaches the bifurcation point at $\alpha = 0$ the system still has the stable limit cycle L_0. Then for $\alpha < 0$, the stable limit cycle L_0 becomes a two-dimensional invariant torus and some long-period cycles of difference stability appear in this torus.

Chapter 7

Bifurcation Control

Bifurcation control refers to the task of modifying certain bifurcative dynamical behavior of nonlinear systems that is desirable for intended application, by means of designing an appropriate controller. Typical objectives of the bifurcation control include delaying the occurrence of an inherent bifurcation, introducing a new bifurcation phenomena at a preferable time or parameter value, changing the parameter set or values of an existing bifurcation point, modifying the shape or type of a bifurcation chain, stabilizing a bifurcated solution or branch, monitoring the multiplicity, amplitude and/or frequency of some limit cycles emerging from a bifurcation mechanism, optimizing the system performance near a bifurcation point, or a combination of these objectives. In our case, the bifurcation control is intended to force the system to a limit cycle with smaller amplitude or eventually to the desired equilibrium point.

Genesio et. all. [9] gave analytical conditions for bifurcations of limit cycles in the describing function term of parameters for nonlinear feedback systems where the nonlinear element is the feedback loop, as depicted Figure 7.1. The analytical conditions are summarized in the following table.

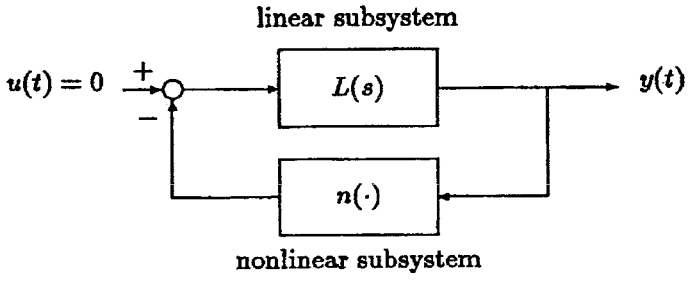

Figure 7.1: Nonlinear Feedback Systems

bifurcation	PLO $y_1(t)$	admissible perturbation $\Delta y(t)$	analytical conditions
1. symmetry breaking	$B\cos\omega t$	ϵ	$N_0' + L^{-1}(0) = 0$
2. cyclic fold	$B\cos\omega t$	$\eta\cos\omega t$	$N_0' + L^{-1}(j\omega) + \frac{1}{2}N_2' = 0$
3. Neimark	$B\cos\omega t$	$\epsilon\cos\omega' t$, $\omega' \neq \frac{\omega}{2}$	$N_0' + L^{-1}(j\omega') = 0$ $\mathrm{Im}\left[L^{-1}(j\omega')\right] = 0$
4. cyclic fold	$A + B\cos\omega t$	$\epsilon + \eta\cos\omega t$	$\left\|N_0' + L^{-1}(0)\right\| \left\|N_0' + L^{-1}(j\omega) + \frac{1}{2}N_2'\right\| = \frac{1}{2}N_1'^2$
5. Neimark	$A + B\cos\omega t$	$\epsilon\cos\omega' t + \eta\cos[(\omega - \omega')t + \theta]$	$\left\|N_0' + L^{-1}(j\omega')\right\| \left\|N_0' + L^{-1}(j(\omega - \omega'))\right\| = \frac{1}{4}N_1'^2$ $\arg\left[N_0' + L^{-1}(j\omega')\right] = \arg\left[N_0' + L^{-1}(j(\omega - \omega'))\right]$
6. flip	$A + B\cos\omega t$	$\epsilon\cos(\omega' t + \theta)$, $\omega' = \frac{\omega}{2}$	$\left\|N_0' + L^{-1}(j\omega')\right\|^2 = \frac{1}{4}N_1'^2$

Figure 7.2: Summary of Limit Cycles Bifurcation Conditions

Bibliography

[1] N.J. Ahmad and F. Khorrami, "Adaptive Control of Systems with Backlash Hysteresis at the Input", *Proc. of the American Control Conference,* San Diego, California, pp. 3018-3022, 1999.

[2] B. Amin and B. Amstrong, *PID Control in the presence of static friction Part II: The reliability of describing function predictions. Technical Report, Dept. of Electrical Eng. and Computer Science, University of Wisconsin, 1994.*

[3] A. Azenha and J.A.T. Machado, "Variable Structure Control of Robots with Nonlinear Friction and Backlash at the Joints", *Proc. of the IEEE Int. Conf. on Robotics and Automation,* Minneapolis, Minnesota, pp. 366-371, 1996.

[4] D.W. Berns, J.L. Moiola and G. Chen, "Feedback Control of Limit Cycle Amplitudes from A Frequency Domain Appraoach", *Automatica,* vol. 34, No. 12, pp. 1567-1573, 1998.

[5] R. Boneh and O. Yaniv, "Reduction of Limit Cycle Amplitude in the Presence of Backlash", *Journal of Dynamic Systems, Measurement, and Control,* Transaction of The ASME, vol. 121, pp. 278-284, June, 1999.

[6] A. Bonsignore, G. Ferretti and G. Magnani, "Coulomb Friction Limit Cycles in Elastic Positioning Systems", *Journal of Dymanic Systems, Measurements, and Control,* Transaction of the ASME, vol. 121, June, 1999.

[7] D.H. Chyung, "Output Feedback Controller for Systems Containing a Backlash", *Proc. of the 31st IEEE Conf. on Decision & Control,* Tucson, Arizona, USA, pp. 3429-3430, 1992.

[8] K. Ezal, P.V. Kokotovic, and G. Tao, "Optimal Control of Tracking Systems with Backlash and Flexibility", *Proc. of the 36th Conf. on Decision & Control,* San Diego, California, USA, pp. 1749-1754, 1997.

[9] R. Genesio and M. Basso and A. Tesi, "Analysis and Synthesis of Limit Cycle Bifurcations in Feedback Systems", *Proc. of the 34th Conf. on Decision & Control,* New Orleans, LA, pp. 2904-2909, 1995.

[10] C. Hatipoglu and U. Ozguner, "Robust Control of Systems InvolvingNon-smooth Nonlinearities Using Modified Sliding Manifolds", *Proc. of the Amarican Control Conf.,* Philadelphia, USA, pp. 2133-2137, 1998.

[11] Y.A. Kuznetsov, *Elements of Applied Bifurcation Theory,* Applied Mathematical Sciences 112, Springer-Verlag, 1995.

[12] J.H.A. van de Laar, *Limit Cycle Behaviour of a Mechanical Servo-system,* Master's Thesis, Report No. WFW 99.008, Fac. of Mechanical Engineering, Eindhoven University of Technology, 1999.

[13] B.C. Lesieutre, A.M. Stankovic and J.R. Lacalle-Melero, "A Study of State Variable Participation in Nonlinear Limit-Cycle Behavior", *Proceedings of the 4th IEEE Conference on Control Applications*, pp. 79-84, 1995.

[14] J.A.T. Machado and A. Azenha, "Position/Force Fractional Control of Mechanical Manipulators", *Advanced Motion Control*, 1998., AMC '98-Coimbra., 5th International Workshop on , pp. 216 -221, 1998.

[15] M.T. Mata-Jimenez and B. Brogliato, "On the Control of Mechanical Systems with Dynamic Backlash", *Proc. of the 36th Conf. on Decision & Control,* San Diego, California, USA, pp. 1990-1995, 1997.

[16] J.L. Moiola and G. Chen, "Controlling the Multiplicity of Limit Cycles", *Proc. of the 37th IEEE Conf. on Decision & Control,* Tampa, Florida, USA, pp. 3052-3057, 1998.

[17] A.H. Nayfeh and B. Balachandran, *Applied Nonlinear Dynamics,* Willey Series in Nonlinear Sciences, John Willey & Sons Inc., 1995.

[18] M. Odai and Y. Hori, " Speed Control of 2-Inertia System with Gear Backlash using Gear Torque Compensator", *Advanced Motion Control*, 1998., AMC '98-Coimbra., 5th International Workshop on , pp. 234-239, 1998. *Proceedings of the 1996 IEEE International Conference on Control Applications*, Dearborn, MI, USA, pp. 798-803, 1996.

[19] H. Olsson and K.J. Astrom, "Friction Generated Limit Cycles", *Proceedings of the 1996 IEEE International Conference on Control Applications*, Dearborn, MI, USA, pp. 798-803, 1996.

[20] M.G. Ortega, J. Aracil, F. Gordillo and F.R. Rubio, "Bifurcation Analysis of a Feedback System with Dead Zone and Saturation", *IEEE Control Systems Magazine,* pp. 91-101, August, 2000.

[21] C.J. Radcliffe and S.C. Southward, "A Property of Stick-Slip Friction Models which Promotes Limit Cycle Generation", *Proc. of the Amarican Control Conf.,* San Diego, California, USA, pp. 1198-1203, 1990.

[22] S.M. Shahruz and S.A. Rajarama, "Suppression of Limit Cycles in a Class of Non-Linear Systems by Disturbance Observers", *Journal of Sound and Vibration, 229 (4),* pp. 1003-1012, 2000.

[23] A.T. Shenton, "Parameter Space Design of PID Limit Cycle Controllers", *Proc. of the Amarican Control Conf.,* San Diego, California, USA, pp. 3342-3346, 1999.

[24] G. Tao and P.V. Kokotovic, "Continous-Time Adaptive Control of Systems with Unknown Backlash", *IEEE Transaction on Automatic Control,* vol. 40, No. 6, pp. 1083-1087, 1995.

[25] G. Tao and P.V. Kokotovic, "Adaptive Control of Systems with Unknown Output Backlash", *IEEE Transactions on Automatic Control,* vol. 40, No. 2, pp. 326-330, 1995.

[26] A. Tesi, E.H. Abed, R. Genesio and H.O. Wang, "Harmonic Balance Analysis of Period-doubling Bifurcations with Implications for Control of Nonlinear Dynamics", *Automatica,* vol. 32, No. 9, pp. 1255-1271, 1996.

[27] H. Wang and M. Krstic, " Extremum Seeking for Limit Cycle Minimization, *Proc. of the 37th IEEE Conf. on Decision & Control,* Tampa, Florida, USA, pp. 2438-2442, 1998.